Journal of Biomedical Materials Research Part B: Applied Biomaterials

WILEY

Society For Biomaterials

RESEARCH ARTICLE OPEN ACCESS

In Vitro Evaluation of Biomaterials for Heart Valve Prosthesis: High Hydrostatic and Enzymatic Treatments as Alternative for Bio-Derived Materials

Danila Vella[1] | Parnaz Boodagh[2,3,4] | Laura Modica De Mohac[1] | Sang-Ho Ye[2,3] | Federica Cosentino[1] | Federica Scaglione[1] | Sofia Dei Bardi[1] | Giulia Polizzi[1] | Garrett Coyan[2,5] | William R. Wagner[2,3,4] | Gaetano Burriesci[1,6,7] | Antonio D'Amore[1,2,3,4,8]

[1]Ri.MED Foundation, Palermo, Italy | [2]McGowan Institute for Regenerative Medicine, Pittsburgh, Pennsylvania, USA | [3]Department of Surgery, University of Pittsburgh, Pittsburgh, Pennsylvania, USA | [4]Department of Bioengineering, University of Pittsburgh, Pittsburgh, Pennsylvania, USA | [5]Children's Hospital of Philadelphia, Philadelphia, Pennsylvania, USA | [6]UCL Mechanical Engineering, University College London, London, UK | [7]Department of Engineering, University of Palermo, Palermo, Italy | [8]Medicina di Precisione in Area Medica, Chirurgica e Critica, University of Palermo, Palermo, Italy

Correspondence: Antonio D'Amore (adamore@fondazionerimed.com)

Received: 16 October 2024 | **Revised:** 25 April 2025 | **Accepted:** 29 April 2025

Funding: The study was funded by Adeka corporation (Japan). Adeka had the opportunity to review the raw data prior to publication but had no editorial oversite or input into the preparation of this manuscript.

Keywords: cardiac prosthetic biomaterials | prosthetic heart valve durability | prosthetic heart valve hydrodynamics | thrombogenicitycalcification

ABSTRACT

Various biomaterials are currently used in clinical settings for heart valve repair and replacement. However, the optimal tissue preparation technique remains elusive. In this study, a non-crosslinked tissue obtained from bovine pericardium, developed by Adeka Corporation, was compared with three commercially-available tissues: two fixed tissues obtained from crosslinked bovine pericardium, CryoLife PhotoFix and LeMaitre CardioCel, and an unfixed one obtained from swine intestinal submucosa, CorMatrix CorPatch. The four biomaterials were used to produce aortic valve prostheses, and their hydrodynamic performance and durability were evaluated according to the ISO5840 standards. Resistance to calcification was evaluated by exposing the tissue to simulated body fluids, followed by SEM and Micro-CT analysis. Thrombogenicity was investigated by exposing the tissue to fresh ovine blood, followed by imaging with SEM and quantifying platelet deposition with lactate dehydrogenase assay. All constructed valves were compliant with the ISO5840 for hydrodynamic assessment. Non-crosslinked tissues, Adeka and CorPatch, showed lower durability but exhibited improved in vitro performances in the simulated biological environments compared to fixed ones. The Adeka tissue demonstrated significantly lower calcium ($p < 0.05$, Adeka vs. CardioCel, PhotoFix) and platelet deposition ($p < 0.05$, Adeka vs. CardioCel, CorPatch, PhotoFix), along with improved durability compared to the other unfixed tissue (Adeka 357,198 vs. CorPatch 0 cycles). In vitro experiments indicate that the crosslinked tissues, CardioCel and PhotoFix, provided mechanical strength adequate to withstand the operating conditions required for heart valve tissue applications. Whilst the Adeka material, a non-crosslinked tissue surrogate, provides improved properties in terms of resistance to calcification and thrombus formation.

Danila Vella and Parnaz Boodagh contributed equally to this study.

1 | Introduction

Bioprosthetic heart valve implantation is increasingly becoming the valve replacement modality of choice for patients affected by valvopathies, representing approximately 80% of surgical prostheses currently implanted [1]. This is largely motivated by the superior hemodynamics provided by flexible leaflets and by less stringent anticoagulation requirements compared to mechanical heart valves. Yet, bioprosthetic leaflet dysfunction, primarily due to calcific degradation, limits the long-term success of this technology [2–4].

Commercially available bioprosthetic valve leaflet tissue is primarily derived from bovine pericardium, porcine aortic valves or pericardium, or bovine jugular vein treated with crosslinking agents such as glutaraldehyde, or fixatives such as those utilized for the cardiac patch CardioCel [5] that are adopted to control the rate of degradation and improve mechanical properties [6, 7]. Although these treatments have the ability to provide structural improvements, they remain inadequate to deplete immunogenic and xenogeneic carbohydrate antigens, which are, in turn, responsible for chronic inflammation and calcific nodule formation that may lead to long-term valve failure [8]. These mechanisms are strictly influenced by the chemical compositions, the physio-mechanical properties, and 3D architecture of the biomaterials [9]. A broad variety of different processing methods for heart valve leaflet surrogates have been proposed, including biological tissue decellularization, electrospinning, 3D bioprinting, hydrogel molding, or cell sheet stacking [10]. Among these, decellularization has been recognized as potentially ideal for generating valve leaflets with adequate mechanical properties, resistance to thrombus formation, and a suitable environment for cell infiltration [11].

Adeka Corporation (Tokyo, Japan) has developed a non-crosslinked cardiac tissue replacement alternative composed of decellularized bovine pericardium treated with both a physical process involving high hydrostatic pressure and an enzymatic treatment, aiming at preserving the micro-architecture of the original material. In order to comparatively assess the newly developed cardiac tissue surrogate, here called Adeka, three clinically available patches that are currently adopted for cardiac repair were selected to undergo testing as heart valve tissue; these included: CardioCel (LeMaitre, Burlington, MA), a glutaraldehyde crosslinked patch made of bovine pericardium [12]; PhotoFix (CryoLife, Kennesaw, GA) a photo oxidized bovine pericardium [13]; and CorPatch (CorMatrix Cardiovascular Inc., Roswell, GA, USA), a composite patch made of four layers of lyophilized small intestine submucosa (SIS) [14]. The primary aim of this study was to comparatively assess the suitability and

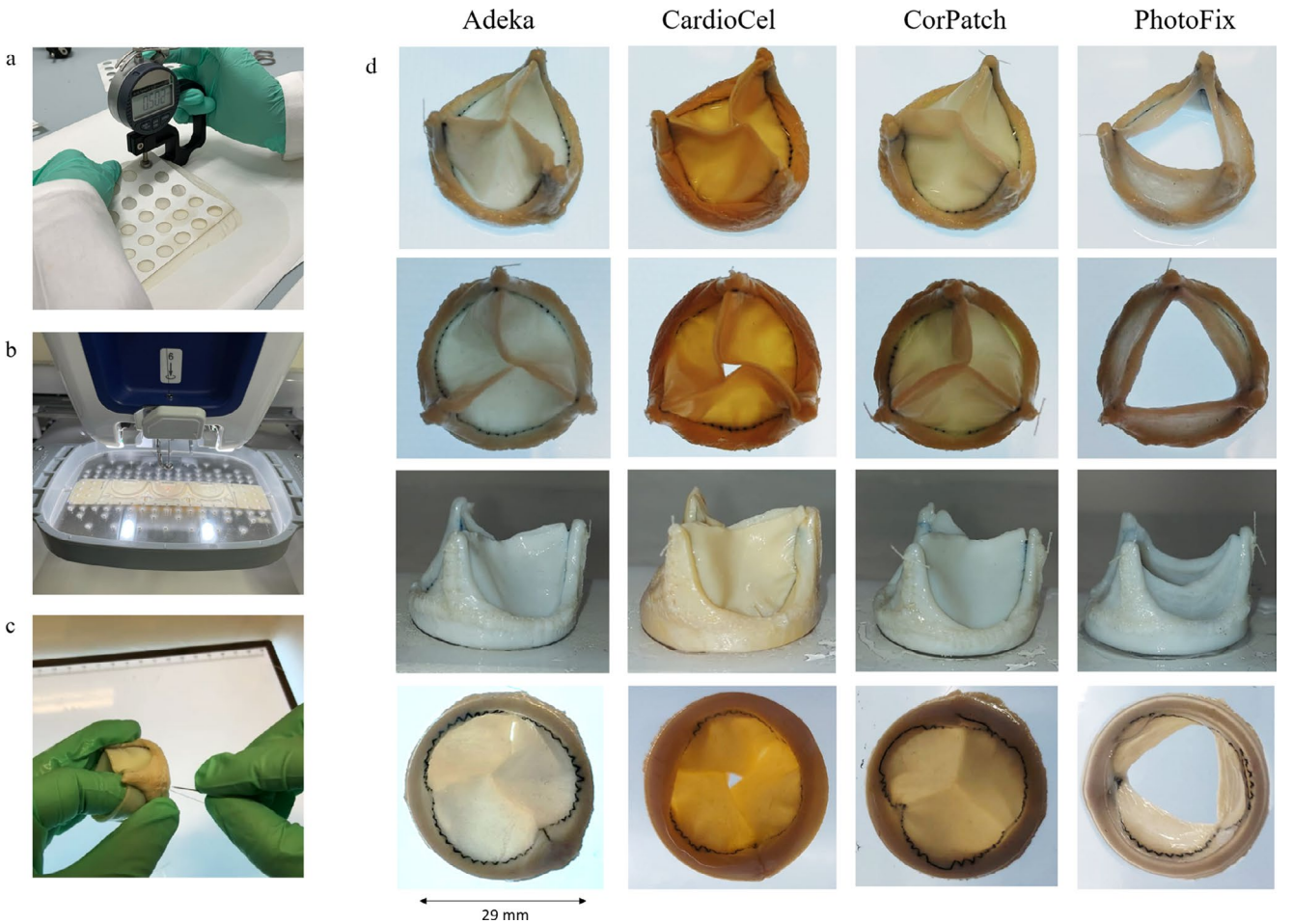

FIGURE 1 | Valve fabrication, main steps. (a) Mechanical caliper thickness measurements to select tissue regions that are more suitable as valve leaflet. (b) Automatic suture of the three-pointed crown profile of the leaflet attachments. (c) Hand-made suturing of the valve leaflets on the stent. (d) Representative fabricated valves, from top to bottom: Fully closed valve, outflow view, front view and inflow view.

performance of these four materials for the fabrication of aortic valve prosthesis. Our hypothesis was that the different processing approaches utilized to process the biomaterials induce different functional outcomes in terms of hydrodynamics, durability, thrombogenicity, and calcification.

2 | Materials and Methods

2.1 | Valve Prosthesis Fabrication

Four stented prosthetic aortic valves were fabricated with each of the four different biomaterials considered for this study (Adeka, CardioCel, PhotoFix and CorPatch) following the procedure described in detail by Rahmani et al. [15]. A total of four samples were obtained, one valve per tissue type. The valve leaflets as well as the stent frame covering sheet were obtained from two patches of the same type of tissue, joined together by a zig-zag suture line along the leaflet base. The patches were selected for fabrication after evaluating four different features: thickness, optical homogeneity, fiber orientation, and elasticity. Patch thickness was quantified using a digital micrometer; several points, horizontally and vertically spaced 20 mm from each other, were considered (Figure 1a). The obtained values were translated into a heat map (Matlab R2020a) in order to better identify regions suitable for valve leaflet manufacturing. Patches with the lowest global scores were selected to be used for the stent frame covering layer, which requires lower mechanical strength. All the patches were stored at room temperature in phosphate buffered saline (PBS) solution for the entire duration of the fabrication and testing process.

To minimize structural variability and operator influence during valve manufacturing, the zig-zag suture defining the leaflet profile was obtained with a computer-controlled automatic suturing machine (VR Embroidery Machine, Brother), see Figure 1b. A second sheet was then used to cover the Delrin stents (diameter 29 mm) and affixed by manual suturing (Figure 1c). Each valve prosthesis was exposed to a hydrostatic pressure of 4 mmHg to verify its ability to achieve full closure prior to further testing.

2.2 | Hydrodynamic and Durability Assessment

All of the heart valve prototypes underwent in vitro hydrodynamic testing in a pulse duplicator system (ViVitro Superpump, SP3891, Canada) via standard testing protocol in compliance with ISO 5840 [16] (see Video S1). The pulse duplicator system, adopted in this study, is composed of three cardiac chambers connected by exchangeable heart valves and filled with a circulating fluid controlled by a volumetric pump. An electromagnetic flowmeter (Carolina Medical, USA) and pressure transducers (Utah Medical, USA) allow for the recording of hydrodynamic parameters. The experiments were conducted at room temperature using PBS as the test fluid. The valve performances were evaluated at cardiac outputs in the range of 2–7 lpm, except for the CorPatch valve, which was tested for reduced cardiac outputs in the range of 2–5 lpm in order to avoid introducing further damage prior to the durability assessment. This decision was supported by the regurgitant fraction vs. cardiac output and transvalvular pressure vs. cardiac output diagrams that indicated a substantial departure from the expected progression when reaching 5 lpm, which corresponds to healthy standard operating conditions. In fact, the presence of this level of leakage is not well sustained at higher cardiac outputs, as the systolic ejection fraction needs to be substantially increased from the nominal value to compensate for the regurgitant flow. Hence, although the valve did not present observable signs of degradation prior to high cycle testing, data from the hydrodynamic testing suggested that it was close to its limit operating conditions.

After hydrodynamic assessment via the pulse duplicator system, valve prototypes were placed in a High Cycle System (BDC Laboratories VDT-3600i CO, USA) to evaluate durability through accelerated wearing testing performed at a 10 Hz cycle rate at room temperature. The valves were mounted on test chambers, filled with PBS with 1 g/L of sodium azide as a fungicide/bactericide. The system software records only the cycles where pressure conditions comply with the ISO 5840 requirements, that is, the valve is exposed for more than 5% of each cycle to a pressure higher than 100 mmHg. The valves were daily inspected by observation under stroboscopic light to detect signs of damage and were functionally evaluated every 40 million cycles (corresponding to 1 year) by repeating the hydrodynamic test protocol in the pulse duplicator system according to ISO 5840.

2.3 | Assessment of Calcium Formation

The response of the different patch materials to calcification was assessed by evaluating calcium deposition after prolonged immersion in two selected fluids with different ionic composition. The first test fluid, simulated body fluid (SBF) was based on the ISO 2,3317 [17]. Although it is not specifically mentioned for valve simulations and is recommended for the assessment of implant materials intended to come into direct contact with bones, its ion concentrations are similar to those detected in human blood plasma.

The second fluid (named: “E” in this study) was based on the work presented by Kiesendahl et al. [18], and was specifically designed for the assessment of the calcification potential on bovine pericardium patches used for heart valve fabrication.

A sample support was built by laser cutting Plexiglas sheets, and was designed to host all patch samples, maintain vertical orientation, and ensure consistency and repeatability when exposing the samples to the calcification agents. Consistent with the conditions utilized to store the patch materials, Adeka and CorPatch samples were provided dry, whereas CardioCel and PhotoFix were hydrated and supplied in PBS solution. Two square samples with a side of 10 mm per each patch type were utilized to test exposure to each of the two fluids. Details on sample exposure to the fluids are fully described in Supplementary Section 1. After the calcification test, samples were dried and each sample was subdivided into four strips, obtaining a total of 16 samples per tissue type. Eight samples underwent qualitative analysis via scanning electron microscopy and energy dispersive X-ray spectroscopy (SEM-EDS, Phenom Pro X, Thermo Fisher Scientific), and 8 samples underwent quantitative analysis via computed

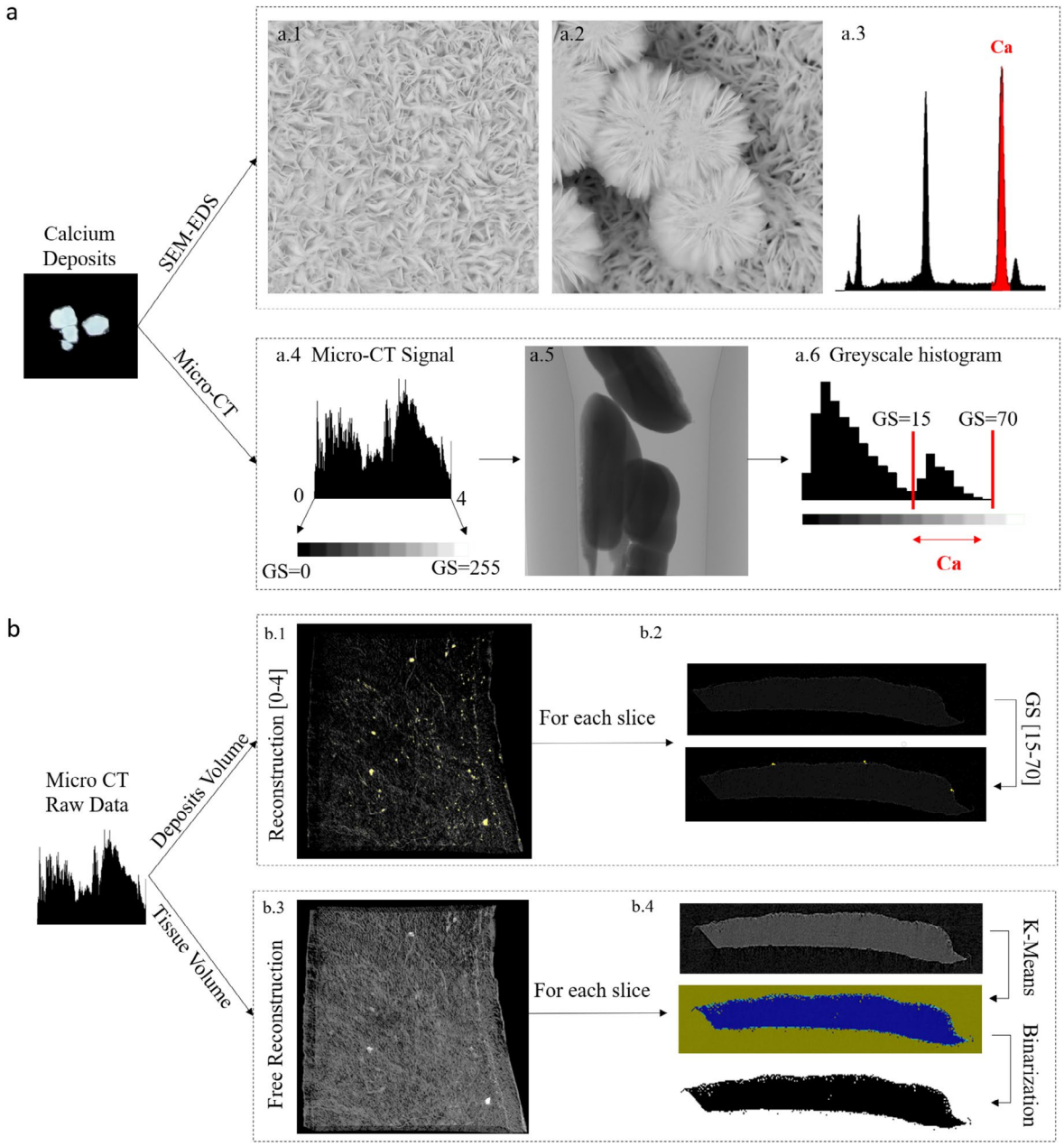

FIGURE 2 | Calcification test. (a) Calcium deposits were isolated after the calcification test and analyzed by two different techniques. SEM-Element Detection Signal (EDS) was used to verify their chemical composition: Representative Octacalcium Phosphate SEM images (a.1, a.2) and associated EDS spectrum a.3. Micro-CT data were processed using the selected thresholds equal to [0–4] (a.4) for volume reconstruction of the calcium deposits (a.5), which was then used to identify the greyscale (GS) range specifically associated to the calcium [15–70] (a.6). (b) Matlab algorithm designed to detect the volume of the calcium deposits and the volume of whole sample tissue based on micro-CT data. The micro CT raw data were processed to obtain two different reconstructions: Using the reference range [0–4] (b.1), each slice is processed for the deposit volume extraction, based on the previously identified greyscale values [15–70] (b.2); using a free range to optimize the tissue visualization (b.3), each slice is analyzed by k-means clustering and binarized to detect whole sample volume (b.4).

tomography with 1.5 μm resolution (micro-computed tomography [micro-CT], Bruker). In order to quantify calcium deposition, based on Micro-CT raw data, a specific protocol was designed (Figure 2) where the tissue volume and the calcium volume detected in each micro-CT scan were used to calculate the percentage of calcium deposits. In detail, calcium phosphate deposits, found in the jars utilized in the tests and verified by SEM-EDS, were used as reference to identify the specific greyscale values associated with calcium deposits. Finally, the percentage of calcium deposits was calculated as the ratio of the calcium volume to the tissue volume found in each sample by means of a specific Matlab code. Full details on the calcification test are provided in Supplementary Section 1 and Supplementary Figures S1 to S5.

2.4 | Assessment of Platelet Deposition

Thrombotic deposition on patch samples was assessed by exposing the materials to citrated fresh ovine blood on a rocking

plate for 2 hours. Whole ovine blood was collected by jugular venipuncture. NIH guidelines for the care and use of laboratory animals were observed, and all animal procedures were approved by the Institutional Animal Care and Use Committee at the University of Pittsburgh. The patch surface was observed by SEM (JSM-6330F, JEOL USA Inc., Peabody, MA) after fixing the surface-adherent platelets and then serially dehydrating with solutions of increasing ethanol content (from 50% to 100% with a step of 10% increments). Deposited platelets on each surface were also quantified by a lactate dehydrogenase (LDH) assay with an LDH Cytotoxicity Detection Kit (Clontech Laboratories Inc. Mountain View, CA); further details are provided in Supplementary Section 2.

2.5 | Statistics

All the data in this manuscript are expressed as mean ± standard deviation. Statistical analysis was conducted by ANOVA followed by post hoc Neuman-Keuls test. To analyze the calcium percentages obtained from the micro-CT scans, a linear regression model was utilized and set with two independent variables: the tissue type (the main factor of interest) and the calcification fluid (the factor associated with the experimental setting). The analyses were conducted using the R software. A value of $p \leq 0.05$ was considered significant.

3 | Results

3.1 | Thickness Mapping for Valve Prosthesis Fabrication

Patch thickness varied substantially between the 4 sample groups: 0.37 ± 0.083 mm for Adeka, 0.393 ± 0.06 mm for CardioCel, 0.458 ± 0.096 mm for PhotoFix, and 0.233 ± 0.025 mm for CorPatch ($p < 0.03$ between all pairs). Adeka, CardioCel, and PhotoFix exhibited large thickness inhomogeneities between different regions of the same patch, while CorPatch presented a more homogeneous patch thickness (Figure 3). These thickness maps were used to identify the patch samples offering homogeneous regions of thickness in the range between 0.375 and 0.425 mm, which were considered suitable for the manufacturing of the prosthetic aortic valve leaflets utilized for the material functional assessment.

3.2 | Aortic Valve Prosthesis Hydrodynamic Assessment

Pulse duplicator hydrodynamic assessments confirmed compliance with all valve requirements specified in ISO 5840 at the start of the experiment, exhibiting regurgitant fraction below 20% and an Effective Orifice Area (EOA) above 2.25 cm [2] at a standard physiological cardiac output of 5 L/min (Figure 4). All of the valves exhibited a similar behavior at 5 L/min in terms of main performance parameters such as mean systolic transvalvular pressure (Δp), closing and leakage volumes, and energy loss (forward + closing) (Figure 4b).

3.3 | Valve Prosthesis Durability

Valve prostheses were subsequently positioned into the High Cycle System for durability assessment (Figure 5). The CorPatch valve failed during the test set-up due to delamination and fracture of the leaflets. Interestingly, inspection of the valve after failure revealed that leaflets had failed at their belly region, while the free edges preserved their structural continuity. Moreover, no fracture was observed at the support anchoring regions, indicating that the damage that led to failure was not associated with the presence of sutures and therefore can be related to inadequate capacity of the material to withstand flow and pressure regimens acting in the aortic valve position. Durability testing was then performed with

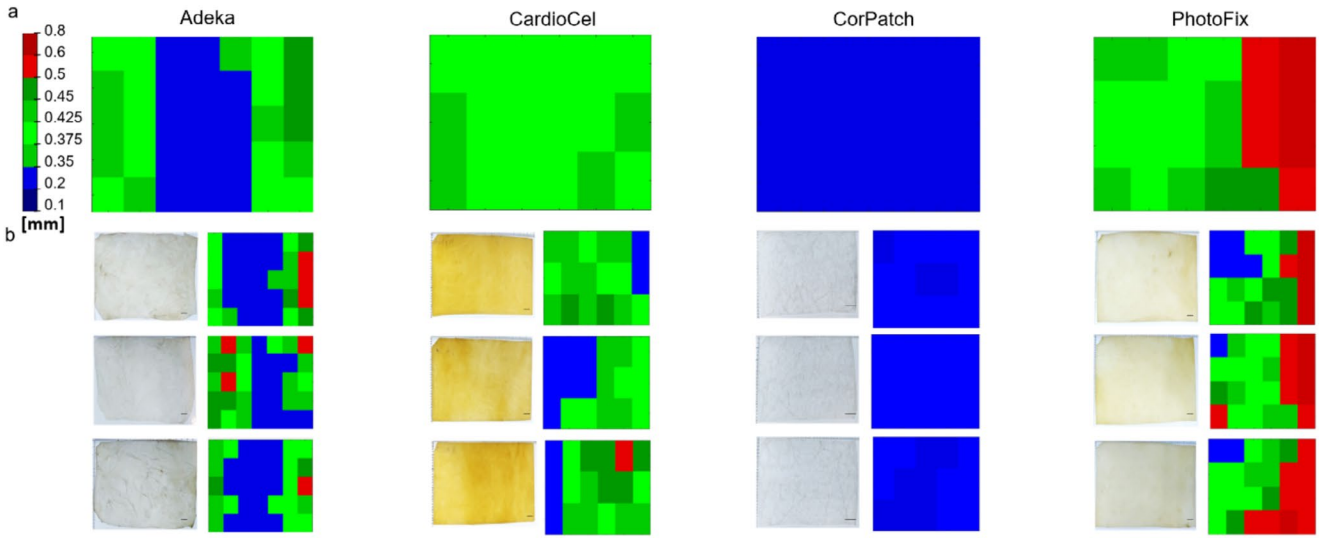

FIGURE 3 | Thickness mapping. Adeka, CardioCel, CorPatch, and PhotoFix patch materials. The green colors indicate the suitable range for leaflets manufacturing, blue colors indicate thickness that are too thin while red colors indicate thickness values that are too thick and therefore not suitable for leaflets manufacturing. (a) Averaged map ($n = 3$ and 35 points for Adeka, $n = 5$ and 18 points for CardioCel, $n = 5$ and 15 points for CorPatch, $n = 5$ and 24 points for PhotoFix) of the thickness measurements. (b) Representative images of the patches observed under light transmission (left) and their associated thickness maps, the reference bar at the bottom of each image indicates the length 1 cm.

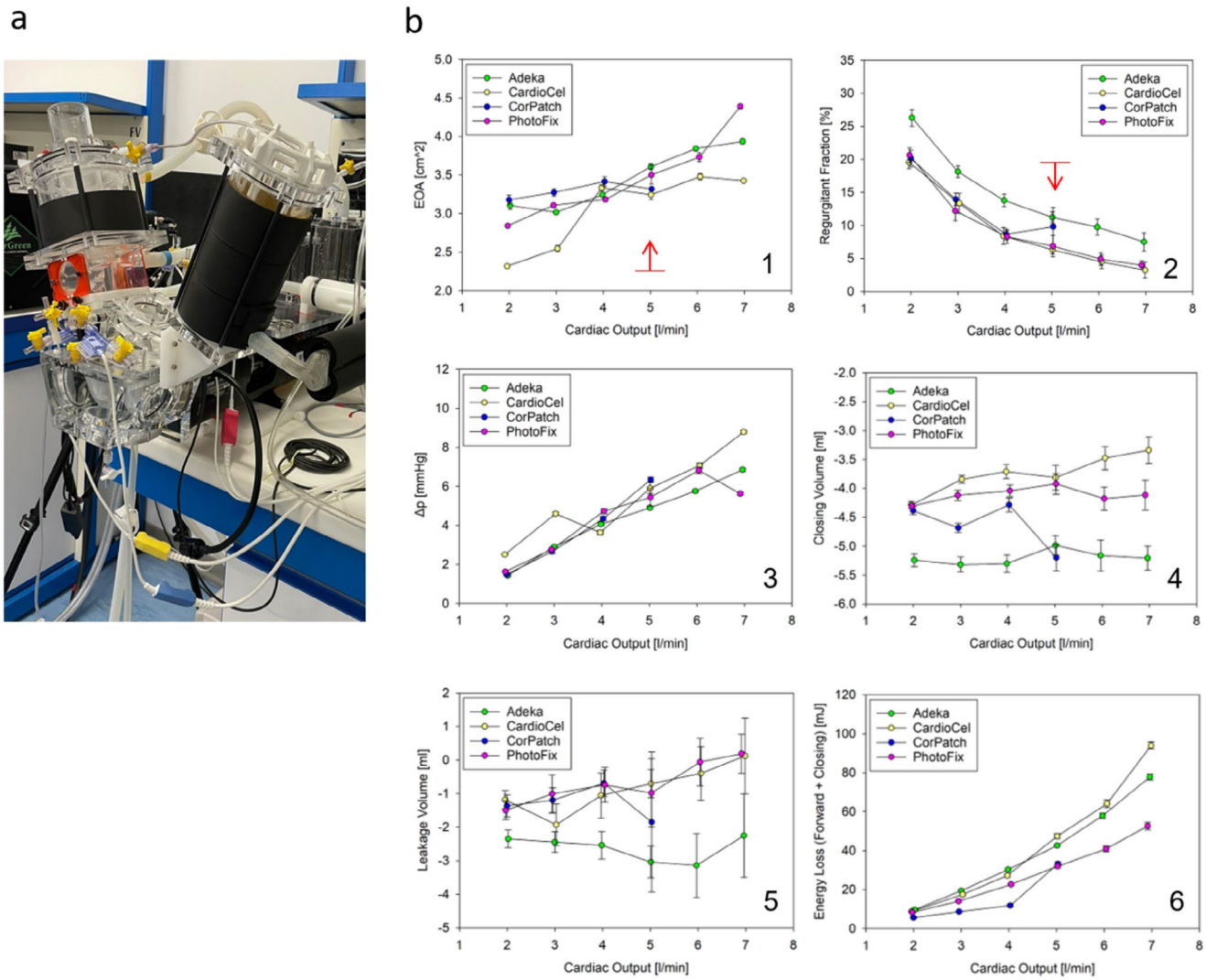

FIGURE 4 | Hydrodynamics assessment. (a) ViVitro System used for the hydrodynamic performance evaluation. (b) Valve performance evaluation included: Engineering Orifice Area (EOA) (1), regurgitant fraction (2), mean systolic transvalvular pressure (3), closing (4) and leakage volume (5), energy loss (forward + closing) (6). The red arrows highlight the limits required by ISO 5840 [16].

the other three surviving valves: Adeka, PhotoFix, and CardioCel. The Adeka valve failed after 357,198 cycles due to prolapse of one of the leaflets, which in turn was caused by a puncture in the proximity of one of the commissures (Figure 5a).

Hydrodynamic performance of the CardioCel and PhotoFix valves was re-assessed after 40 million cycles (1 year equivalent) in the pulse duplicator. The effect of cycling on the CardioCel valve resulted in a significant increase in the EOA (from 3.24 ± 0.06 cm [2] to 4.46 ± 0.09 cm [2]), with a stable regurgitant fraction (from 6.3% ± 0.66% to 6.71% ± 0.8%). Increases in the EOA were also observed for the PhotoFix valve (from 3.5 ± 0.12 cm [2] to 4.44 ± 0.08 cm [2] at 5 L/min), although this was counterbalanced by a major increase in the regurgitant fraction (from 6.84% ± 1.64% to 25.85% ± 2.16% at 5% L/min), which made the valve unable to meet the minimum operating regulatory standards (Figure 5b) at 40 million cycles. Yet, as the valve did not show observable damage, and adequate operating conditions could be potentially regained in the durability test, durability assessment was continued for a larger number of cycles for both devices.

The PhotoFix valve failed after 73,535,888 cycles, due to a tear developed in proximity to one of the commissures (Figure 5a). The durability test was then continued on the only surviving valve, the CardioCel, up to 120 million cycles. Specifically, this valve did not show any sign of damage at any stage of the durability test. Visual observation of the Adeka and PhotoFix leaflets indicated considerable stretching of the leaflets, which appeared considerably deformed when compared to their original design shape (Figure 5a).

3.4 | Assessment of Calcium Deposition

The deposit areas as well as the total count of the calcium deposits identified by SEM/EDS are reported in Figure 6a,b. The qualitative analysis suggests that, based on deposit area and number, CardioCel and PhotoFix are more prone to calcium deposit formation; in particular, CardioCel seems to lead to several deposits of small size (high count and low area), while PhotoFix seems to lead to fewer deposits of larger size (middle count and high area).

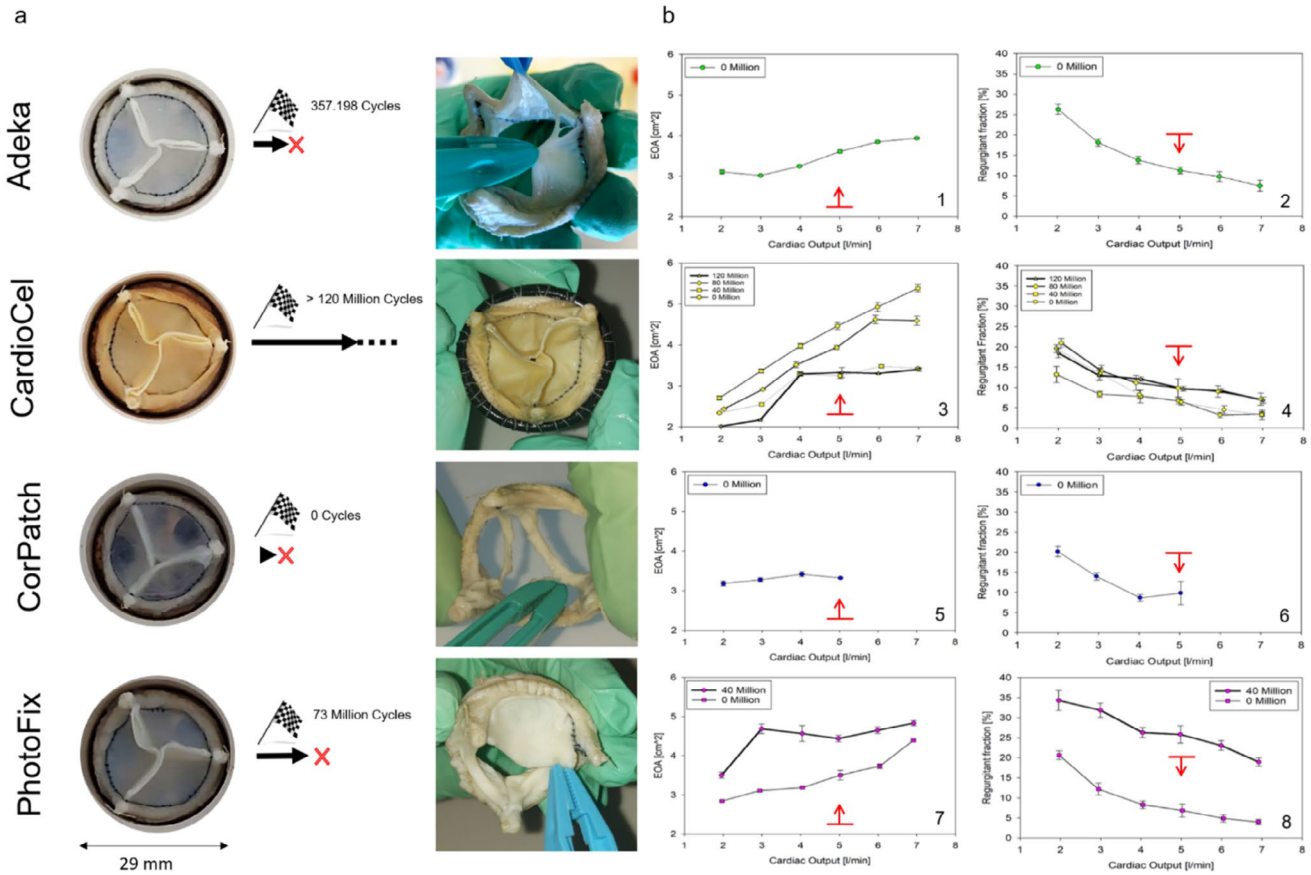

FIGURE 5 | Durability assessment. (a) From left to right: The four operating valves (captured in closed configuration), the number of cycles reached by each valve type before any structural damage occurred, only CardioCel successfully passed > 120 M cycles. (b) hydrodynamics performance graphs evaluated at the following cycles: Adeka EOA (1) and regurgitant fraction (2) at 0 million; CardioCel EOA (3) and regurgitant fraction (4) at 0 million, 40 million, 80 million, 120 million; CorPatch EOA (5) and regurgitant fraction (6) at 0 million; PhotoFix EOA (7) and regurgitant fraction (8) at 0 million, 40 million.

Visual inspection of the 3D volumes obtained by micro-CT analysis corroborated the SEM-EDS analysis (Supplemental Figures S4 and S5) with CardioCel and PhotoFix showing more deposits than the Adeka and CorPatch patches. Consistent with the SEM-EDS analysis, PhotoFix was affected by the largest calcium deposits that were notably visible in samples treated with SBF fluid (Supplemental Figure S5). CardioCel showed mostly deposits of smaller size than PhotoFix, especially in samples treated with fluid E (Supplemental Figure S4).

Calcium deposits were also quantified as deposit volume/sample volume fraction. For all text samples ($n = 8$/group) (Figure 6c,d). The average fraction computed for the four groups was $0.004 \pm 0.003\%$ for Adeka, $0.015 \pm 0.009\%$ for CardioCel, $0.004 \pm 0.003\%$ for CorPatch, and $0.017 \pm 0.017\%$ for PhotoFix. Statistical analysis resulted in significant differences among the bioprosthetic tissues ($p < 0.05$) and no significant differences between the two calcification fluids ($p = 0.69$). The post hoc comparison indicated that Adeka was significantly different from PhotoFix ($p < 0.05$) and CardioCel ($p < 0.05$).

3.5 | Platelet Deposition

Through both LDH and SEM assessments, Adeka showed the lowest platelet deposition compared to the other three patches (Figure 7). The LDH testing (Figure 7a) confirmed visual LDH observations; the amount of platelet deposition on Adeka's samples was statistically lower than the other patch types ($p < 0.05$, Adeka vs. CardioCel, CorPatch or PhotoFix, $n = 7$), and the difference between the control samples was not significant. Platelet deposition was also estimated by visually counting in images acquired through the SEM (Figure 7b). Overall, Adeka patches showed lower platelet deposition than the other patch groups, confirming the results obtained by the LDH test. The thrombotic deposition assessment performed via SEM demonstrated that the Adeka patch had lower platelet deposition compared to CardioCel and PhotoFix ($p < 0.001$ for each), while no significant difference was detected compared to CorPatch (Figure 7c). Most interestingly, Figure 7d compared the effect of patch surface on platelet deposition; all four patch materials were more thrombogenic on the rougher sides. For each group of patches, the smooth side presented a significantly lower platelet deposition than the rough side (Adeka and CorPatch with $p < 0.001$, CardioCel with $p < 0.01$), except for the PhotoFix patch ($p > 0.05$). This finding suggests that the rough side is more prone to deposits such as calcium or platelet accumulation, due to the exposure of radicals in the collagen molecules.

Overall, this result suggests that the smooth side of the Adeka patch has the lowest platelet deposition.

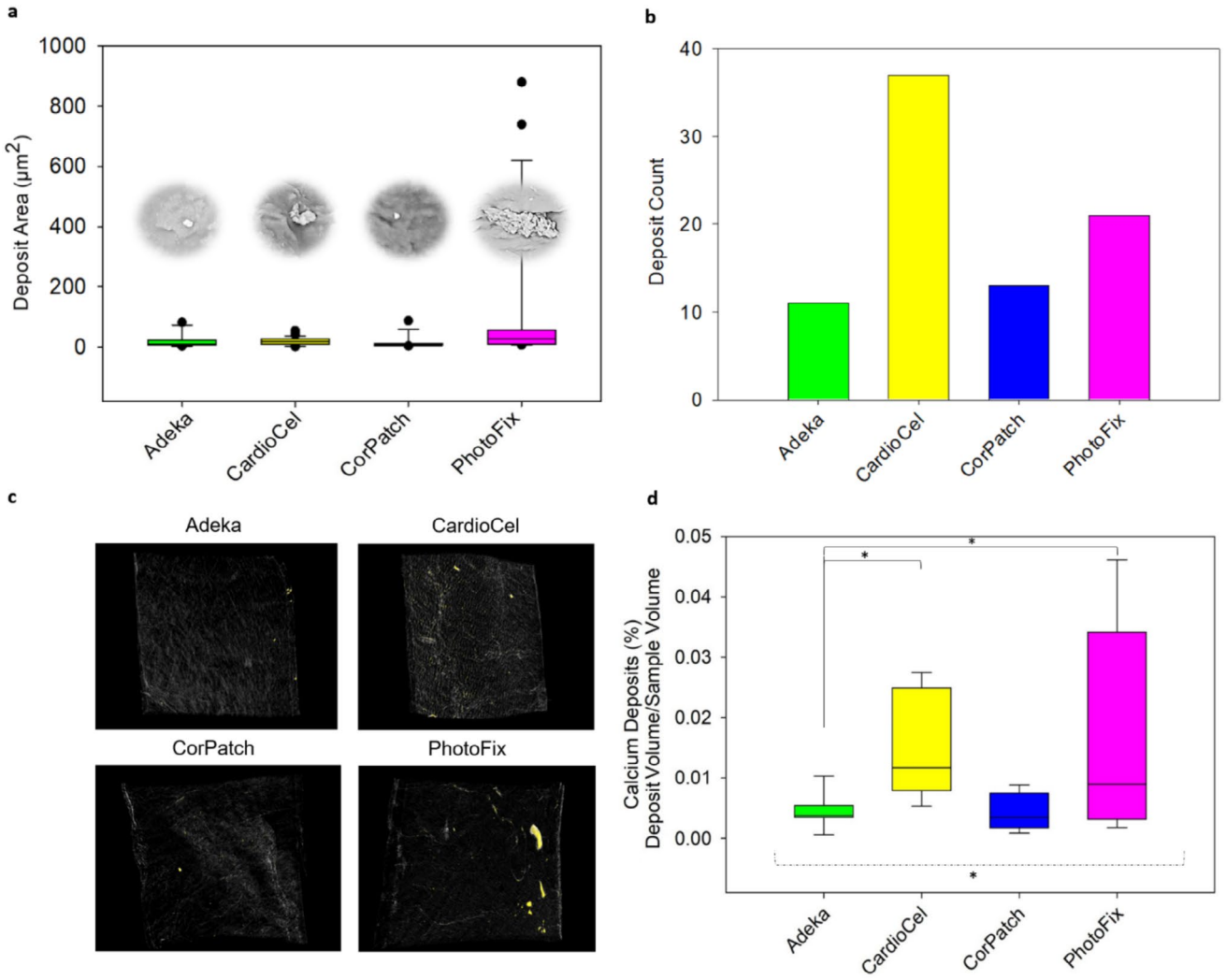

FIGURE 6 | Calcification test. (a) Mean area of calcium deposits as identified by SEM-EDS. Representative pictures of the deposits are provided for each tissue type. (b) Total count of the calcium deposits identified by SEM-EDS. (c) Representative image stacks (0.5 mm [3]) of the micro-CT data for the four patch types after being exposed to the calcification fluids: The yellow pixels indicate the calcium deposits detected. (d) Calcium deposit volume fraction quantified via Matlab post-processing of the micro-CT data. Data are presented as mean ± std. ANOVA (dot line) and, post hoc comparisons (continuous line) were performed, with * indicating a $p < 0.05$.

4 | Discussion

Manufacturing processes adopted for materials that are designed for cardiovascular repair should be able to either prescribe adequate mechanical properties or, when applied to biology-derived materials, preserve structural features that characterize native healthy, functional tissue. Similarly, an ideal manufacturing process should provide or maintain adequate bioactivity to elicit favorable biological interaction with the host environment. More specifically for prosthetic heart valve applications, favorable host-biomaterial interactions include avoiding thrombus formation, biochemical alterations, and any form of tissue degeneration dictated by progressive structural damage, calcium deposition, tissue overgrowth, or leaflet thinning.

Commonly used decellularized, biologically derived materials for cardiac repair are processed with crosslinking treatments, aimed at depleting immunogenic and xenogeneic antigens and improving their mechanical strength and durability. However, the fixation process itself compromises native microarchitecture and, as a consequence, affects function and the interactions with the host physiology [19–21]. This limitation is conceptually addressed through two primary approaches: (I) advancing synthetic biomaterials with controlled structure–function, enhanced durability, and the major advantage of not being affected by xenogeneic factors [22] and (II) developing better processing and chemical fixation strategies for biologically derived materials [23, 24].

As the interest for synthetic materials increases with polymeric heart valve prostheses being approved or under clinical trial (e.g., SIKELIA valve by MitrAssist Lifesciences Limited [25], Foldax Tria [26] clinical trial ID NCT04717570, InFlow [27]), an equal investment is still underway in identifying innovative processing techniques able to preserve native micro-architecture, mechanics and bioactivity of pericardium native tissue [28]. In

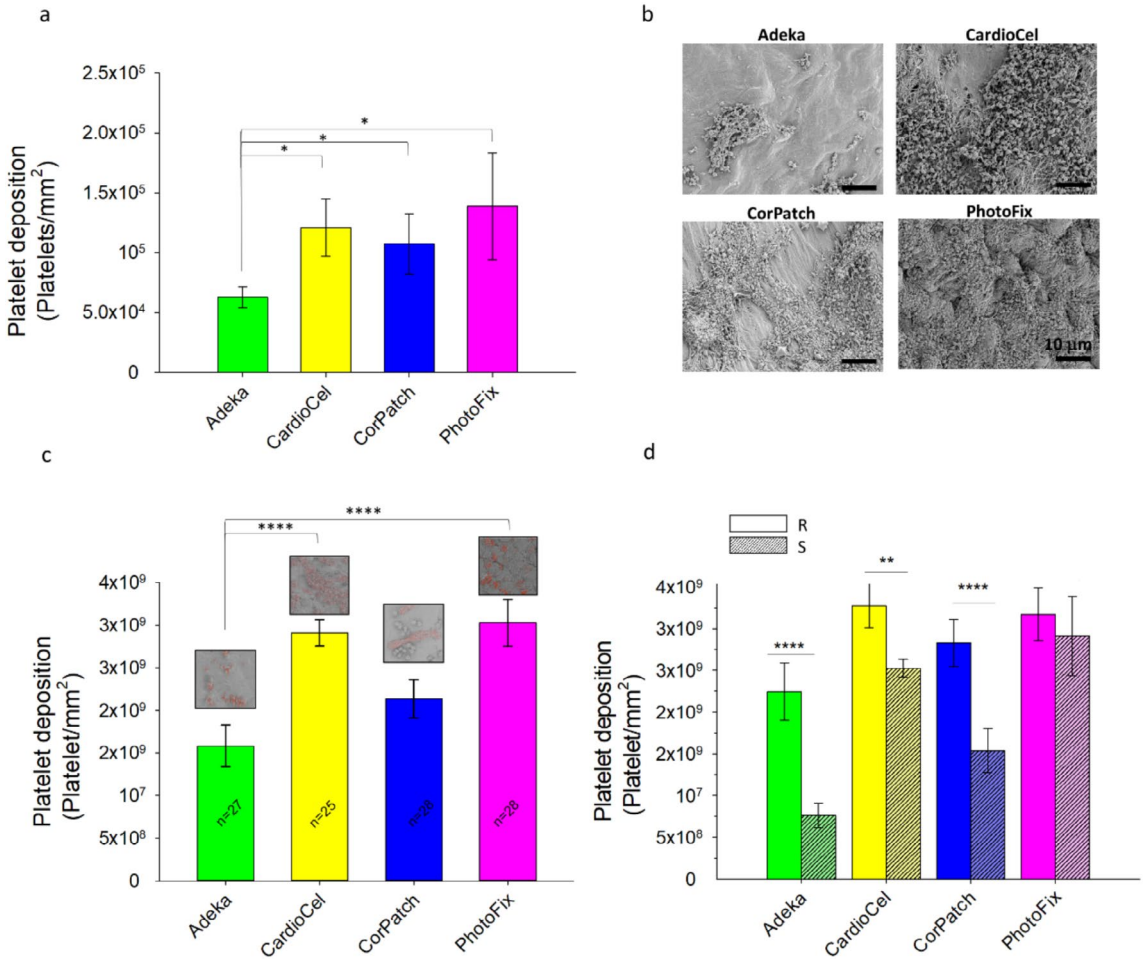

FIGURE 7 | Assessment of platelet deposition. (a) Assessment of platelet deposition ($n = 7$) via lactate dehydrogenase (LDH) assay, the analysis was performed on both the S and the R side. (b) Representative SEM images of platelet deposition on Adeka, CardioCel, CorPatch and PhotoFix patch material. (c) Platelet deposition expressed as the average platelets/mm [2] detected via analysis of scanning electron microscopy (SEM) images of both the smooth and rough sample sides. (d) Platelet deposition via analysis of SEM images, platelet count has been performed separately on the smooth (S) and rough (R) side ($n = 7$). *indicating a $p < 0.05$; **indicating a $p < 0.01$, and ****indicating a $p < 0.001$.

this study, the Adeka patch, a newly developed non-crosslinked biomaterial, processed with high hydrostatic pressure and enzymes, is compared with other clinically available cardiac patches: CorPatch and two crosslinked patches, CardioCel and PhotoFix.

CardioCel and PhotoFix are state of the art crosslinked materials able to provide good durability and mechanical strength and, as such, are currently adopted both for prosthetic heart valve manufacturing and valve repair [5, 29–31]. Examples includethe Ozaki procedure [30], the Ross-Konno procedure [32], cusp extension [33], or the neocuspidization [34]. CorPatch, in contrast, is an unfixed material and is characterized by a relatively intact extracellular matrix architecture that appeared to be functional to promote angiogenesis and suitable for surgical revascularization [35]. CorPatch is also used for heart valve reconstruction and repair, although its efficacy for this use is supported primarily by animal studies and clinical reports with a small number of patients and a short follow-up [36].

To address the performance of these biomaterials for valve manufacturing, four identical stented aortic valve prostheses were produced and then their ability to operate under pressure and flow conditions typical of the cardiac cycle was evaluated. Thickness is an indicator of patches suitability for valve manufacturing. In detail, thickness values in the range 0.35–0.5 mm are ideal to obtain valve leaflets able to experience the highest stress levels during the valve operating cycle. Instead, tissue too thin or too thick or tissue characterized by thickness inhomogeneity could negatively impact valve operating, potentially leading to early failure. Thickness values and homogeneity were evaluated in equidistant regions of the patches (Figure 3). Adeka exhibits thickness in the range 0.37 ± 0.083 mm. CardioCel showed an average thickness of 0.393 ± 0.06 mm, which was consistent with the literature and the manufacturer's specification [37]; similarly, PhotoFix reported a larger thickness than CardioCel (0.458 ± 0.096 mm) as also expected based on [38]. Instead, CorPatch thickness resulted to be the lowest, with a value of 0.233 ± 0.025 mm (the patch is sold as a composite of 4 lyophilized sheets [14]); this value was slightly lower than the one reported in literature [22]. This difference may be due to the reduced number of points and the reduced area evaluated (in this study 15 points over 70 cm [2] were considered, whereas in Sun et al. [22] only 3 points in 0.28 cm [2] were measured).

Adeka, CardioCel, and PhotoFix exhibited large thickness inhomogeneities between different regions of the same patch, while CorPatch presented lower percentage variations. Despite the greater uniformity, this tissue was substantially thinner than the others, and the minimum target thickness (0.375 mm) for the leaflet could not be met.

Benchtop mechanical tests characterizing the mechanical response of the four materials were recently published in the study by Boodagh et al. [39]. Among the patches, CardioCel appeared to be the most rigid, making it easier to handle but at the same time more difficult to stretch to tightly fit with the stent. Moreover, the higher puncture resistance made it harder to suture. On the contrary, CorPatch was the softest material, which made it particularly difficult to handle, but easier to suture and to wrap around the stent. Adeka and PhotoFix patches exhibited similar handling features, with resistance to the needle puncture and ease of handling intermediate between CardioCel and CorPatch; this makes these tissues particularly suitable for the conventional industrial manufacturing which is still heavily dependent on human operators. Despite these differences, all of the assessed biomaterials were adequate to build valve prototypes for this study. Hydrodynamic tests (Figure 4) indicated that all valves met the minimum regulatory requirements (e.g., EOA above 2.25 cm [2] and regurgitant fraction below 20%), with similar functional parameters. When assessed for durability (Figure 5), only CardioCel could reach an estimated durability superior to three equivalent years, maintaining functionality. In fact, both unfixed tissues failed early (in the first stages of the test the CorPatch, and after few hundred thousand cycles the Adeka), while the PhotoFix was unable to maintain minimum hydrodynamic performance at the 40 million cycles assessment. The layering characteristic of the CorPatch tissue is the likely cause of failure, as delamination may result from the transvalvular pressure difference being applied to individual thin layers, unable if isolated to withstand physiologically relevant pressure values. These results suggested that the Adeka tissue structure is weaker than the two crosslinked materials (CardioCel and PhotoFix), but superior to the other non-crosslinked tissue, CorPatch. Also, this result agrees with the finding that the thickness of the Adeka patch is closer to that of the fixed patches. Despite the agreement between hydrodynamic test and thickness analysis, it should be noted that just one valve per tissue type was used for the tests. This limits the generalizability of the presented findings. Comparison of these data with the existing literature cannot be provided as this is the first ever presented comparative study on these four biomaterials.

The host-patch interaction was assessed in vitro by focusing on two specific factors that are relevant for valve leaflet application: resistance to calcium deposition and thrombus formation. Calcium deposit accumulation (Figure 6) was evaluated by exposing the tissue to two simulated body fluids [17, 18] and was evaluated both qualitatively via SEM-EDS and quantitatively by micro-CT. To quantify calcium presence from micro-CT raw data, a specific protocol was designed. Both quantitative and qualitative results identified the unfixed tissues, Adeka and CorPatch, as less prone to calcification. More specifically, Adeka tissue resulted in differences against crosslinked tissues, both PhotoFix and CardioCel. These results were in agreement with the literature, as glutaraldehyde cross-linking treatments generally make bioprosthetic tissues more prone to calcification [24, 40, 41]. In contrast, unfixed SIS tissue is more resistant to calcification; for instance, Scholl et al. [42] reported that calcific degeneration was not observed in 40 patients who underwent cardiac reconstructions with SIS. Baird et al. [43] evaluated photo-oxidized treatments in vivo and reported that this class of treatments makes pericardium less prone to calcification than glutaraldehyde, although numerous cases of calcified valves were observed [13]. The reduced calcification measured in the Adeka patch represents an important advantage for potential applications of this tissue for heart valve prosthesis manufacturing. Calcification remains the primary cause of premature failure in bioprosthetic heart valves, significantly affecting performance and long-term durability [2, 3]. This limitation has taken on greater relevance in recent years, since surgical valve replacement is becoming a treatment option also for younger patients [5], a group characterized by accelerated calcification kinetics of bioprosthesis [19, 44].

Last, resistance to thrombus formation (Figure 7) was studied by analyzing platelet deposition after exposure to fresh ovine blood and further evaluated qualitatively via SEM and quantitatively via lactate dehydrogenase (LDH) test. Reduced platelet deposition was observed for the Adeka patch when compared to the other three groups. The Adeka smooth side provided the lowest deposition when compared to all of the other samples. This was consistent with the known influence of surface topology and rugosity on platelet deposition and activation [45]. Overall, the results suggested that Adeka and CorPatch are the most favorable options due to their significantly reduced platelet deposition on the patch surface.

Recapitulating host cell infiltration was out-of-scope for this report, and in particular cannot be modeled with ISO standard functional and durability tests (valves are tested in simple saline solution, with fungicide); therefore, nothing can be speculated in terms of host cell infiltration or tissue elaboration. Despite this limitation, tests conducted in simulated biological conditions showed that unfixed patches, Adeka and CorPatch, demonstrated the lowest calcium and platelet deposition, suggesting a good potential for favorable integration with the host in vivo.

5 | Conclusion

The comprehensive set of in vitro tests conducted in this study aimed to investigate two major factors that are considered critical for heart valve leaflet material: I) the functional and tissue mechanical properties, in terms of hydrodynamics and durability; and II) the resistance to the two major host-biomaterial interaction complications: calcification and thrombus formation. Processing, fixing, and preparation methodologies for decellularized biomaterials assessed in this work and potentially utilized for heart valve repair and replacement differed substantially in their ability to withstand mechanical and biochemical stimuli in a physiologically relevant in vitro environment, confirming the leading hypothesis of the study. Most importantly, when the results of this comparative assessment of these four commercial materials are translated to the broader class of

processing they belong to, it can be stated that: crosslinked tissues (CardioCel and PhotoFix) generally provide mechanical strength adequate to withstand the demanding operating conditions associated with heart valve tissue applications. Whereas, the non-crosslinked materials (CorPatch and Adeka) offer improved properties in terms of resistance to calcium and thrombus formation. Within this specific category of materials, those processed with high hydrostatic pressure and an enzymatic treatment (Adeka) can provide additional value in terms of function, durability, and resistance to platelet deposition and calcification. While incremental, this processing method could serve as a promising alternative, if durability is further improved, for biologically derived heart valve leaflet manufacturing.

Disclosure

Dr. D'Amore, Dr. Coyan, and Dr. Wagner are shareholders of Neoolife Inc.

Conflicts of Interest

The authors declare no conflicts of interest.

Data Availability Statement

The data that support the findings of this study are available from the corresponding author upon reasonable request.

References

1. S. J. Head, M. Çelik, and A. P. Kappetein, "Mechanical Versus Bioprosthetic Aortic Valve Replacement," *European Heart Journal* 38, no. 28 (2017): 2183–2191, https://doi.org/10.1093/EURHEARTJ/EHX141.

2. O. Barannyk, R. Fraser, and P. Oshkai, "A Correlation Between Long-Term In Vitro Dynamic Calcification and Abnormal Flow Patterns Past Bioprosthetic Heart Valves," *Journal of Biological Physics* 43, no. 2 (2017): 279–296, https://doi.org/10.1007/s10867-017-9452-9.

3. B. Zhang, E. Salaun, N. Côté, et al., "Association of Bioprosthetic Aortic Valve Leaflet Calcification on Hemodynamic and Clinical Outcomes," *Journal of the American College of Cardiology* 76, no. 15 (2020): 1737–1748, https://doi.org/10.1016/j.jacc.2020.08.034.

4. J. J. Bax and V. Delgado, "Bioprosthetic Heart Valves, Thrombosis, Anticoagulation, and Imaging Surveillance," *JACC: Cardiovascular Interventions* 10, no. 4 (2017): 388–390, https://doi.org/10.1016/J.JCIN.2017.01.017.

5. D. Bell, K. Betts, R. Justo, et al., "Multicenter Experience With 500 CardioCel Implants Used for the Repair of Congenital Heart Defects," *Annals of Thoracic Surgery* 108, no. 6 (2019): 1883–1888, https://doi.org/10.1016/J.ATHORACSUR.2019.04.085.

6. J. E. Valentin, A. M. Stewart-Akers, T. W. Gilbert, and S. F. Badylak, "Macrophage Participation in the Degradation and Remodeling of Extracellular Matrix Scaffolds," *Tissue Engineering, Part A* 15, no. 7 (2009): 1687–1694, https://doi.org/10.1089/TEN.TEA.2008.0419.

7. W. Kong, C. Lyu, H. Liao, and Y. Du, "Collagen Crosslinking: Effect on Structure, Mechanics and Fibrosis Progression," *Biomedical Materials* 16, no. 6 (2021): 062005, https://doi.org/10.1088/1748-605X/AC2B79.

8. E. S. Fioretta, S. E. Motta, V. Lintas, et al., "Next-Generation Tissue-Engineered Heart Valves With Repair, Remodelling and Regeneration Capacity," *Nature Reviews. Cardiology* 18, no. 2 (2021): 92–116, https://doi.org/10.1038/s41569-020-0422-8.

9. W. M. L. Neethling, K. Puls, and A. Rea, "Comparison of Physical and Biological Properties of CardioCel With Commonly Used Bioscaffolds," *Interactive Cardiovascular and Thoracic Surgery* 26, no. 6 (2018): 985–992, https://doi.org/10.1093/icvts/ivx413.

10. M. Li, H. Wu, Y. Yuan, B. Hu, and N. Gu, "Recent Fabrications and Applications of Cardiac Patch in Myocardial Infarction Treatment," *Viewpoints* 3, no. 2 (2022): 20200153, https://doi.org/10.1002/viw.20200153.

11. D. Sharma, M. Ferguson, T. J. Kamp, and F. Zhao, "Constructing Biomimetic Cardiac Tissues: A Review of Scaffold Materials for Engineering Cardiac Patches," *Emergent Materials* 2, no. 2 (2019): 181–191, https://doi.org/10.1007/s42247-019-00046-4.

12. W. M. L. Neethling, S. Yadav, A. J. Hodge, and R. Glancy, "Enhanced Biostability and Biocompatibility of Decellularized Bovine Pericardium, Crosslinked With an Ultra-Low Concentration Monomeric Aldehyde and Treated With ADAPT," *Journal of Heart Valve Disease* 17, no. 4 (2008): 456–463. accessed February 20, 2023, https://europepmc.org/article/med/18751476.

13. C. A. Svendsen, N. S. Kreykes, J. Butany, et al., "In-Vivo Assessment of a Photofixed Bovine Pericardial Valve," *Journal of Heart Valve Disease* 9, no. 6 (2000): 813–820. accessed January 24, 2023, https://europepmc.org/article/med/11128791.

14. V. Vasanthan, M. Biglioli, A. F. Hassanabad, J. Dundas, R. G. Matheny, and P. W. M. Fedak, "The CorMatrix CorTM PATCH for Epicardial Infarct Repair," *Future Cardiology* 17, no. 8 (2021): 1297–1305, https://doi.org/10.2217/FCA-2021-0017.

15. B. Rahmani, C. McGregor, G. Byrne, and G. Burriesci, "A Durable Porcine Pericardial Surgical Bioprosthetic Heart Valve: A Proof of Concept," *Journal of Cardiovascular Translational Research* 12, no. 4 (2019): 331–337, https://doi.org/10.1007/S12265-019-09868-3.

16. International Standard, *ISO 5840-1:2015 (E): Cardiovascular implants: cardiac valve prostheses* (ISO Copyright Office, 2015).

17. Implants for Surgery–In vitro Evaluation for Apatite-Forming Ability of Implant Materials, ISO 23317.

18. N. Kiesendahl, C. Schmitz, M. Menne, T. Schmitz-Rode, and U. Steinseifer, "In Vitro Calcification of Bioprosthetic Heart Valves: Test Fluid Validation on Prosthetic Material Samples," *Annals of Biomedical Engineering* 49, no. 2 (2021): 885–899, https://doi.org/10.1007/s10439-020-02618-6.

19. A. A. Patukale, J. Davies, S. Marathe, N. Alphonso, and P. Venugopal, "Calcification Causing Failure of Tissue Engineered Bovine Pericardium After Aortic Valve Repair," *World Journal for Pediatric and Congenital Heart Surgery* 13, no. 2 (2022): 251–253, https://doi.org/10.1177/21501351211036407.

20. Z. Konakci K, B. Bohle, R. Blumer, et al., "Alpha-Gal on Bioprostheses: Xenograft Immune Response in Cardiac Surgery," *European Journal of Clinical Investigation* 35, no. 1 (2005): 17–23, https://doi.org/10.1111/j.1365-2362.2005.01441.x.

21. C. S. Park, S.-S. Oh, Y. E. Kim, et al., "Anti-Alpha-Gal Antibody Response Following Xenogeneic Heart Valve Implantation in Adults," *Journal of Heart Valve Disease* 22, no. 2 (2013): 222–229, http://www.ncbi.nlm.nih.gov/pubmed/23798212.

22. M. Sun, M. Elkhodiry, L. Shi, et al., "A Biomimetic Multilayered Polymeric Material Designed for Heart Valve Repair and Replacement," *Biomaterials* 288 (2022): 121756, https://doi.org/10.1016/j.biomaterials.2022.121756.

23. F. Naso, U. Stefanelli, E. Buratto, et al., "Alpha-Gal Inactivated Heart Valve Bioprostheses Exhibit an Anti-Calcification Propensity Similar to Knockout Tissues*," *Tissue Engineering, Part A* 23, no. 19–20 (2017): 1181–1195, https://doi.org/10.1089/TEN.TEA.2016.0474.

24. Y. Liu, Z. Wu, C. Chen, et al., "The Hybrid Crosslinking Method Improved the Stability and Anti-Calcification Properties of the Bioprosthetic Heart Valves," *Frontiers in Bioengineering and Biotechnology* 10 (2022): 1008664, https://doi.org/10.3389/fbioe.2022.1008664.

25. J. Ge, D. Zhou, X. Zhang, et al., "Preliminary Implantation of a Novel TAVR Device With Polymeric Leaflets for Symptomatic Calcific Aortic Disease," *JACC Case Reports* 17 (2023): 101901, https://doi.org/10.1016/j.jaccas.2023.101901.

26. S. J. Yakubov, J. Wittel, and G. Johnson, "CRT-700.20 Foldax TRIA TAVI: A Novel-Polymer Transcatheter Aortic Valve: Pilot Chronic Ovine Model Study," *JACC: Cardiovascular Interventions* 15, no. 4 (2022): S59–S60, https://doi.org/10.1016/j.jcin.2022.01.228.

27. M. Kachel, P. P. Buszman, K. P. Milewski, et al., "Temporal, Biomechanical Evaluation of a Novel, Transcatheter Polymeric Aortic Valve in Ovine Aortic Banding Model," *Frontiers in Cardiovascular Medicine* 9 (2022): 977006, https://doi.org/10.3389/fcvm.2022.977006.

28. C. McGregor, G. Byrne, B. Rahmani, E. Chisari, K. Kyriakopoulou, and G. Burriesci, "Physical Equivalency of Wild Type and Galactose α 1,3 Galactose Free Porcine Pericardium; a New Source Material for Bioprosthetic Heart Valves," *Acta Biomaterialia* 41 (2016): 204–209, https://doi.org/10.1016/j.actbio.2016.06.007.

29. E. Talman and J. Poehlmann, "Mechanical Strength of PhotoFix and Glutaraldehyde Treated Porcine Aortic Valve Wall Tissue," in *ASME International Mechanical Engineering Congress and Exposition (IMECE) Proceedings* (American Society of Mechanical Engineers, 2021), 95–96, https://doi.org/10.1115/IMECE1999-0394.

30. S. C. Chivers, C. Pavy, R. Vaja, C. Quarto, O. Ghez, and P. E. F. Daubeney, "The Ozaki Procedure With CardioCel Patch for Children and Young Adults With Aortic Valve Disease: Preliminary Experience – A Word of Caution," *World Journal of Pediatric and Congenital Heart Surgery* 10, no. 6 (2019): 724–730, https://doi.org/10.1177/2150135119878108.

31. C. Pavy, G. Michielon, J. L. Robertus, F. Lacour-Gayet, and O. Ghez, "Initial 2-Year Results of CardioCel Patch Implantation in Children," *Interactive Cardiovascular and Thoracic Surgery* 26, no. 3 (2018): 448–453, https://doi.org/10.1093/icvts/ivx295.

32. G. Zalewski, M. Buczyński, M. Kuśmierczyk, et al., "Ross-Konno Procedure as a Rescue Operation in a Newborn With Critical Aortic Stenosis," *Kardiologia Polska* 81, no. 7–8 (2023): 794–795, https://doi.org/10.33963/KP.a2023.0118.

33. P. O. Myers, C. Tissot, J. T. Christenson, M. Cikirikcioglu, Y. Aggoun, and A. Kalangos, "Aortic Valve Repair by Cusp Extension for Rheumatic Aortic Insufficiency in Children: Long-Term Results and Impact of Extension Material," *Journal of Thoracic and Cardiovascular Surgery* 140, no. 4 (2010): 836–844, https://doi.org/10.1016/j.jtcvs.2010.06.036.

34. D. Blitzer, D. LaPar, A. Olds, et al., "Aortic Valve Neocuspidization in a Pediatric Population: An Early Single Center Experience," *Structural Heart* 3 (2019): 152, https://doi.org/10.1080/24748706.2019.1589817.

35. D. Hlaváček, M. Pokorný, P. Ivák, I. Netuka, and O. Szárszoi, "Implantation of Durable Left Ventricular Assist Device in Patient With Postmyocardial Infarction Ventricular Septal Defect," *Journal of Cardiac Surgery* 36, no. 10 (2021): 3944–3947, https://doi.org/10.1111/JOCS.15839.

36. W. J. Wells, "Responsible Innovation," *Journal of Thoracic and Cardiovascular Surgery* 148, no. 5 (2014): 2225–2226, https://doi.org/10.1016/j.jtcvs.2014.09.016.

37. C. P. Brizard, J. Brink, S. B. Horton, G. A. Edwards, J. C. Galati, and W. M. L. Neethling, "New Engineering Treatment of Bovine Pericardium Confers Outstanding Resistance to Calcification in Mitral and Pulmonary Implantations in a Juvenile Sheep Model," *Journal of Thoracic and Cardiovascular Surgery* 148, no. 6 (2014): 3194–3201, https://doi.org/10.1016/j.jtcvs.2014.08.002.

38. S. C. Hofferberth, C. W. Baird, D. M. Hoganson, et al., "Mechanical Properties of Autologous Pericardium Change With Fixation Time: Implications for Valve Reconstruction," *Seminars in Thoracic and Cardiovascular Surgery* 31, no. 4 (2019): 852–854, https://doi.org/10.1053/j.semtcvs.2019.03.001.

39. P. Boodagh, L. M. De Mohac, Y. Hayashi, et al., "Photooxidation Cross-Linked, Glutaraldehyde Cross-Linked, or Enzyme and Hydrostatic Pressure Processed Decellularized Biomaterials for Cardiovascular Repair Do Not Affect Host Response in a Rat Right Ventricular Outflow Flow Tract Reconstruction (RVOT) Model," *Journal of Biomedical Materials Research Part B: Applied Biomaterials* 113, no. 2 (2025): e35529, https://doi.org/10.1002/jbm.b.35529.

40. J. J. Mercuri, J. J. Lovekamp, D. T. Simionescu, and N. R. Vyavahare, "Glycosaminoglycan-Targeted Fixation for Improved Bioprosthetic Heart Valve Stabilization," *Biomaterials* 28, no. 3 (2007): 496–503, https://doi.org/10.1016/j.biomaterials.2006.09.005.

41. K. Kumar, N. Azordegan, M. Durston, et al., "HMG-COA Reductase Inhibitors Do Not Attenuate the Inflammatory Response Associated With Glutaraldehyde-Fixed Bioprosthetic Heart Valve Conduits," *Canadian Journal of Cardiology* 29, no. 10 (2013): S261, https://doi.org/10.1016/j.cjca.2013.07.429.

42. F. G. Scholl, M. M. Boucek, K.-C. Chan, L. Valdes-Cruz, and R. Perryman, "Preliminary Experience With Cardiac Reconstruction Using Decellularized Porcine Extracellular Matrix Scaffold: Human Applications in Congenital Heart Disease," *World Journal for Pediatric and Congenital Heart Surgery* 1, no. 1 (2010): 132–136, https://doi.org/10.1177/2150135110362092.

43. C. W. Baird, P. O. Myers, B. Piekarski, et al., "Photo-Oxidized Bovine Pericardium in Congenital Cardiac Surgery: Single-Centre Experience," *Interactive Cardiovascular and Thoracic Surgery* 24, no. 2 (2016): 240–244, https://doi.org/10.1093/icvts/ivw315.

44. S. F. Saleeb, J. W. Newburger, T. Geva, et al., "Accelerated Degeneration of a Bovine Pericardial Bioprosthetic Aortic Valve in Children and Young Adults," *Circulation* 130, no. 1 (2014): 51–60, https://doi.org/10.1161/CIRCULATIONAHA.114.009835.

45. J. Linneweber, P. M. Dohmen, U. Kerzscher, K. Affeld, Y. Nosé, and W. Konertz, "The Effect of Surface Roughness on Activation of the Coagulation System and Platelet Adhesion in Rotary Blood Pumps," *Artificial Organs* 31, no. 5 (2007): 345–351, https://doi.org/10.1111/j.1525-1594.2007.00391.x.

Supporting Information

Additional supporting information can be found online in the Supporting Information section.